100-watt sonoluminescence generated by 2.5-atmosphere-pressure pulses

Brian Kappus,[1,*] Shahzad Khalid,[1] and Seth Putterman[1,2]
[1]*Department of Physics and Astronomy, University of California Los Angeles, California 90095, USA*
[2]*California Nano-Systems Institute, University of California Los Angeles, California 90095, USA*
(Received 27 October 2010; revised manuscript received 21 March 2011; published 4 May 2011)

A Xenon gas bubble introduced into a vertically suspended steel cylinder is driven to sonoluminescence by impacting the apparatus against a solid steel base. This produces a 150-ns flash of broadband light that exceeds 100-W peak intensity and has a spectral temperature of 10 200 K. This bubble system, which yields light with a single shot, emits very powerful sonoluminescence. A jet is visible following bubble collapse, which demonstrates that spherical symmetry is not necessary to produce sonoluminescence.

DOI: 10.1103/PhysRevE.83.056304 PACS number(s): 78.60.Mq

I. INTRODUCTION

Sonoluminescence is the transduction of sound into light by a bubble undergoing nonlinear pulsations in a fluid. Current studies suggest that the matter in these bubbles is compressed to near-solid densities [1] and reaches extremely high temperatures [2]. The light can be emitted from a single bubble driven acoustically [3–6], by a cloud of bubbles in the near field of an acoustic horn [7,8], by the far field of a plate vibrating at MHz frequencies [2], or from inertial collapses of bubbles grown by tension pulses [9–11]. These methods are limited in their maximum driving pressures, above which instabilities can distort the bubble and reduce emission [12,13]. Here we report observations of a single-shot sonoluminescing system with an acoustically driven collapse and small initial pressure which stays spherical pre-emission. A Xenon bubble is introduced inside a large steel cylinder which is dropped a small distance and impacts a steel base. The strong acoustic pulse traveling upwards in the fluid from the end of the tube following the impact event collapses the bubble and emits sonoluminescence with very high peak power. This approach offers an avenue to higher densities and temperatures than previously achieved.

II. APPARATUS AND METHODS

For this experiment, a 60-cm-tall by 10-cm-diameter 316-stainless-steel cylinder (see Fig. 1) was filled to a height of 40 cm with purified phosphoric acid and suspended 0.7 cm above an equally sized solid steel base using a small electromagnet. Phosphoric acid was chosen for its low vapor pressure [14,15] and its effectiveness in low-frequency sonoluminescence [16]. The acid is prepared by heating it to 100 °C under vacuum with agitation at 50 Hz in a separate glass apparatus designed for this purpose before being transferred to the steel tube under vacuum. This pretreatment both dehydrates the acid to near 100% concentration and removes any dissolved gas. The area in the steel tube above the acid was maintained at 10 mTorr by a dry scroll pump. A 7-cm piece of 316-stainless, 30-gauge needle tubing enters near the base of the apparatus through a sealed port and is bent so that its end is oriented vertically. Outside the tube, the end of the needle was kept under Xenon at a pressure of more than 100 Torr to prevent backflow of acid. A 0.006″ stainless wire was inserted in the needle to reduce gas flow and slow the bubble seeding rate. This arrangement provided a 0.9-mm-radius Xenon bubble approximately once every 5 seconds. The size of the bubble introduced was dictated entirely by the size of the needle and was very consistent from bubble to bubble. A photogate arrangement with a HeNe laser and small photodiode registered when the bubble detached from the needle and, after a fixed delay provided by a delay generator (SRS DG535), current to the electromagnet holding the tube was shut off. Timing was adjusted so that, when the bubble drifted to a point 11 cm above the base (at the center of the observation windows), the tube was released and impacted the steel base below.

In free fall, the bubble experiences little static pressure and expands to 3.5 mm in radius (see Fig. 2). Upon impact, a high-pressure traveling pulse is released into the fluid that collapses the bubble, resulting in emission of an intense flash of broadband light. We measured the light emission using a Hamamatsu H5783-03 photomultiplier tube (PMT) as well as a spectrometer composed of an Acton Spectra Pro 300i with an Acton broadband optical fiber with matching optics and a Princeton Instruments ICCD-MAX Camera. Analysis shows more than 10^{13} photons per flash within a 150-ns-long pulse, which was roughly Gaussian in shape (see inset to Fig. 3).

III. EXPERIMENTAL RESULTS AND DISCUSSION

Spectroscopic analysis shows a featureless broadband spectrum (see Fig. 3). The measured emission intensity is more than 85 W in average power and the best Planck fit to the spectrum data gives a temperature of 10 200 K. The phosphoric acid significantly absorbs wavelengths shorter than 325 nm [17], preventing measurement of the short-wavelength portion of the spectrum. Using the blackbody fit to extrapolate the spectrum below 325 nm and using 150 ns for the pulse width, we calculate an average emitted power of 135 W. This makes it a very powerful sonoluminescence source.

The bubble radii shown in Fig. 2 were measured using a Hamamatsu C4742-98 CCD camera back-lit by a Powertechnology LDCU12/7108 pulsed-infrared diode laser. The diode laser could be gated internally, triggered by a delay generator (SRS DG535) to select a particular moment in phase with a 30-ns exposure. For the growth phase of the bubble motion,

*kappus@physics.ucla.edu

FIG. 1. (Color online) Photograph of the apparatus showing 3 of 6 total viewports.

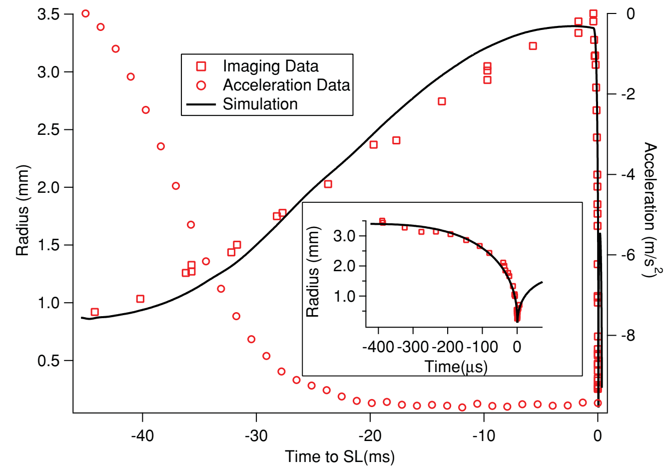

FIG. 2. (Color online) Diagram showing measured radius versus time using backlighting photography. The backlighting was 30-ns exposures using a diode laser captured on a Hamamatsu 14-bit CCD. Timing is shown relative to the sonoluminescence flash. $R_{\min}$ is 94 μm and the maximum surface velocity is 760 m/s, which gives a peak temperature of 270 000 K from the diffusion code. The inset shows the same data and simulation with a magnified time base around the collapse. Also shown is the measured acceleration of the tube as measured by a small IC accelerometer. Phosphoric acid at this concentration has a speed of sound of 1.8×10^5 cm/s and a density of 1.8 g/cm^3.

exposures were a fixed delay from electromagnet release (time $t = 0$). For the collapse phase, a small piezoceramic was attached to the side of the apparatus near the base to provide a timing signal from impact. Bubble images for this collapse phase were taken with delays from this piezo signal.

The Rayleigh-Plesset (RP) equation has been shown to provide a good parametrization of the motion of sonoluminescing bubbles [18]. To diagnose the external pressures experienced by the bubble we used the RP equation including terms for viscosity, surface tension, and acoustic radiation. Due to the low Mach number of the motion of the bubble, we could reasonably model the equation of state of the gas as ideal with uniform pressure. A drop of 0.7 cm that is entirely controlled by gravity and with an instantaneous stop should result in a 7-atm shock wave according $\Delta p = \rho c v$. Our measurements indicate that the release is not perfect and that the shock jump reaches only 2.5 atm. Measurement of the release acceleration is shown in Fig. 2 and is used in the RP model for the growth phase. The collapse was well described by a linearly increasing model of the applied pressure, rising from 0 to 2.5 atmospheres in 450 microseconds (see inset to Fig. 2).

The interior temperature was described by 200 equally spaced Lagrangian radial coordinates with a constant 300-K temperature-bath boundary. This way the internal gas pressure could be accurately modeled as it transitioned from isothermal behavior to adiabatic [19]. Because of the low density of gas from the small ambient pressure and the fast collapse, we calculate that this transition occurs at three times the ambient radius (R_0), which is almost three times larger than is typical with traditional single-bubble sonoluminescence. The interior is also fairly uniform—the model shows that, as the interior heats to double the ambient temperature, nearly 3/4 of the volume stays within 20% of the peak temperature. It is reasonable to assume that this will remain so until the very last moments of collapse when other physics come into play (to be discussed below). While the adiabatic equation of state is regarded as incomplete at $R_{\min}$, it can still provide an estimate of collapse conditions. In this case the model predicts the minimum radius to be 94 μm with a maximum velocity during collapse of 760 m/s. Analyses of the photographs of emission show the collapse radius to be 105 $\pm$ 20 μm, indicating that

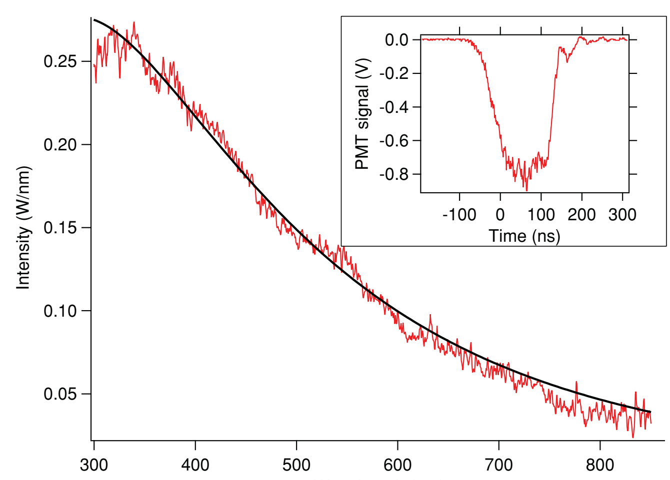

FIG. 3. (Color online) Diagram showing a representative spectrum compiled from 4 separate flashes. The fit is a 10 200-K black body spectrum with an emission radius of 125 μm. This radius is sufficiently close to the measured radius for us to conclude that the emission is that of a black body. The inset is a typical PMT trace.

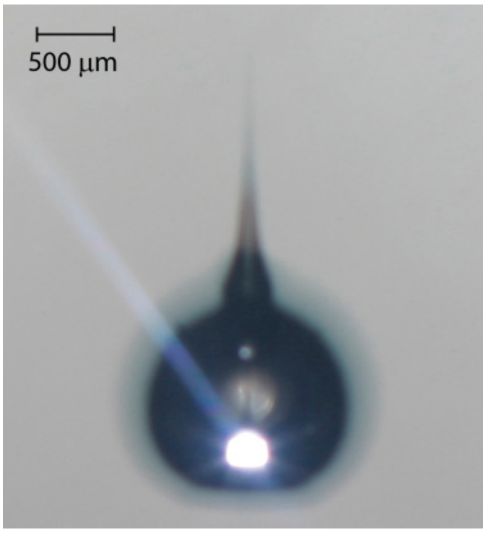

FIG. 4. (Color online) A backlit photograph of the jet formed during collapse. The bright blue light near the bottom of the bubble is the sonoluminescence. The strobe time is 50 μs, which causes considerable blurring in the bubble wall.

the simulation is a reasonable estimate. Using the cross-over radius ($3R_0$), and the measured collapse radius ($105 \pm 20\ \mu$m), we can predict a collapse temperature between 131 000 K ($R_{min} = 125\ \mu$m) and 283 000 K ($R_{min} = 85\ \mu$m).

Such high temperatures are not reached. The conflict between adiabatic predicted temperatures and measured spectroscopic temperatures that we observe is a common aspect of sonoluminescence [16,20,21]. Various physical processes which could play a role in limiting the spectral temperature are: (a) disequilibrium between electrons and ions, (b) cooling by ionization, and (c) jetting inside the bubble. The 150-ns flash width combined with the observed blackbody spectrum suggests that the plasma inside the bubble is in local thermodynamic equilibrium. Also, the calibrated blackbody spectral radius, images of the light emission and the RP simulation of the minimum collapse radius are all within the measurement uncertainty of each other. This suggests that the emission is bubble-filling and opaque [22]. Unifying the adiabatic simulation (94 μm collapse and 250 000 K peak temperature) and Saha's equation of ionization predicts 70 000 K and an average ionization level of 2.4 electrons per atom. This is still too high compared to the measured spectrum.

Nonideality of the ionization process could lead to corrections to the equation of state that result in further cooling. We have suggested in previous work that electrostatic screening and quantum hybridization lower the ionization potential to the point that a "plasma phase transition" yields very high levels of ionization and accounts for the opacity [17,23].

Nonsphericity of the implosion leads to jetting instabilities which are a sink for the mechanical energy. A jet forms during collapse and is clearly visible post-collapse (see Figs. 4 and 5) pointing vertically upward in the liquid column. The jet is first observable 2.5 μs after light emission (see Fig. 5), but could also exist during light emission. These asymmetries decrease the likelihood that a focused shock wave [14] forms inside this bubble.

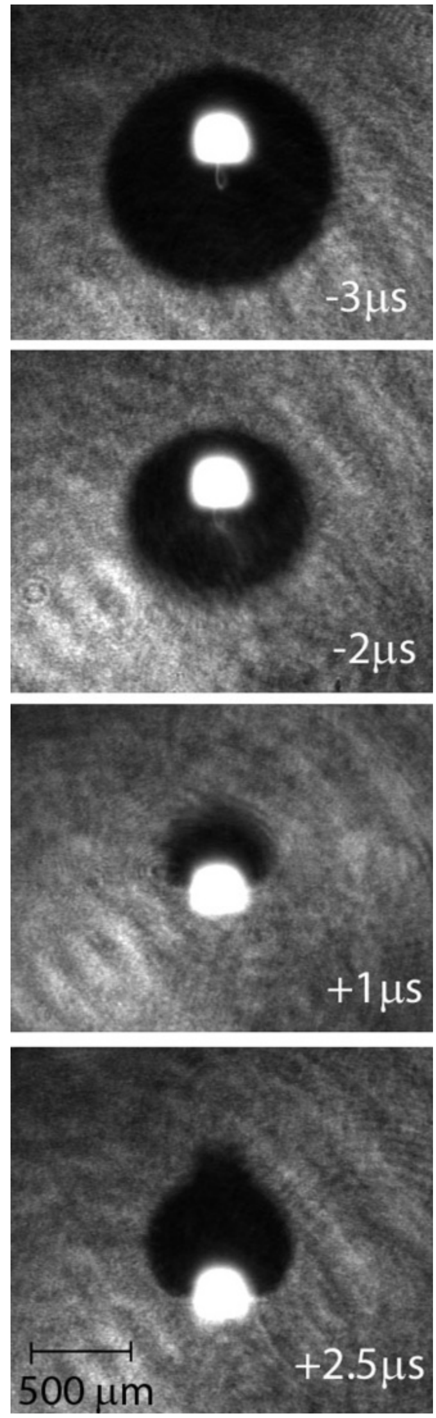

FIG. 5. A series of backlighting images near collapse. Each photo is a 30-ns backlighting exposure. Sonoluminescence is exposed in every photo. In each photo the time relative to the sonoluminescence signal is given. The jet is clearly starting to emerge in the final photo.

In its current form these jetting instabilities limit further increases in the emission. Dropping the tube from a height larger then 0.7 cm greatly diminishes the sonoluminescence and increases the size of the jet. Therefore, we conclude that the instabilities leading to the jet are to blame. A jet forming from this geometry is not surprising [24–27]. Perhaps the instabilities are so intense at the larger drop height that the bubble fragments before necessary temperatures and densities for sonoluminescence are attained. An extension of RP theory to include effects that break the spherical symmetry to allow jetting would predict this case because the collapse velocity of 760 m/s is less than the speed of sound in the acid and the hot Xenon gas.

Changing the symmetry of the high-pressure acoustic wave could prevent jetting in further experiments, paving the way for orders-of-magnitude more pressure and collapse speeds. Nonetheless, even now, this technique represents a dramatic upscaling of sonoluminescence brightness and offers a clear avenue for further study.

ACKNOWLEDGMENTS

This project is supported by DARPA. We thank Carlos Camara for valuable advice regarding all aspects of the project.

[1] K. R. Weninger, B. P. Barber, and S. J. Putterman, Phys. Rev. Lett. **78**, 1799 (1997).

[2] C. Camara, S. Putterman, and E. Kirilov, Phys. Rev. Lett. **92**, 124301 (2004).

[3] P. R. Temple, Master thesis, University of Vermont, 1970.

[4] B. P. Barber and S. J. Putterman, Nature (London) **352**, 318 (1991).

[5] S. D. Hopkins *et al.*, Phys. Rev. Lett. **95**, 254301 (2005).

[6] C. K. Su *et al.*, Phys. of Fluids **15**, 1457 (2003).

[7] T. J. Matula *et al.*, Phys. Rev. Lett. **75**, 2602 (1995).

[8] H. Frenzel and H. Schultes, Zeitschrift Fur Phys. Chemie-Abteilung B-Chemie Der Elementarprozesse Aufbau Der Materie **27**, 421 (1934).

[9] Q. D. Chen and L. Wang, Chinese Phys. **13**, 564 (2004).

[10] Q. D. Chen and L. Wang, Chinese Phys. Lett. **21**, 1822 (2004).

[11] Q. D. Chen and L. Wang, Phys. Lett. A **339**, 110 (2005).

[12] J. L. Thomas, Phys. Rev. E **70**, 016305 (2004).

[13] W. Lauterborn and T. Kurz, Rep. Prog. Phys. **73**, 106501 (2010).

[14] B. D. Storey and A. J. Szeri, Proc. R. Soc. Lon. Series A **456**, 1685 (2000).

[15] R. Toegel *et al.*, Phys. Rev. Lett. **85**, 3165 (2000).

[16] A. Chakravarty *et al.*, Phys. Rev. E **69**, 066317 (2004).

[17] B. Kappus, *Physics* (University Of California, Los Angeles, 2010).

[18] R. Lofstedt, B. P. Barber, and S. J. Putterman, Phys. Fluids A **5**, 2911 (1993).

[19] A. Prosperetti, J. Fluid Mechanics **222**, 587 (1991).

[20] G. Vazquez *et al.*, Phys. Rev. Lett. **88**, 197402 (2002).

[21] S. J. Putterman and K. R. Weninger, Annu. Rev. Fluid Mech. **32**, 445476 (2002).

[22] Y. B. Zel'dovich and Y. P. Raæizer, *Physics of Shock Waves and High-Temperature Hydrodynamic Phenomena* (Dover Publications, Mineola, 2002), p. 27.

[23] B. Kappus *et al.* (submitted work).

[24] T. B. Benjamin and A. T. Ellis, Philosophical Transactions of the Royal Society of London Series A **260**, 221 (1966).

[25] J. P. Dear, J. E. Field, and A. J. Walton, Nature (London) **332**, 505 (1988).

[26] L. A. Crum, Journal De Physique **41**, 285 (1979).

[27] W. Lauterborn and W. Hentschel, Ultrasonics **23**, 260 (1985).